

# Proton- and Reductant-Assisted Dioxygen Activation by a Nonheme Iron(II) Complex to Form an Oxoiron(IV) Intermediate\*\*

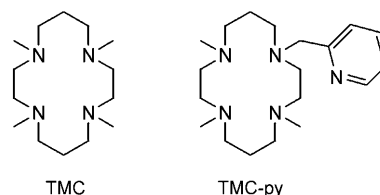
Aurore Thibon, Jason England, Marlène Martinho, Victor G. Young, Jr., Jonathan R. Frisch, Régis Guillot, Jean-Jacques Girerd, Eckard Münck,\* Lawrence Que, Jr.,\* and Frédéric Banse\*

Dedicated to Professor Jan Reedijk

Dioxygen activation by mononuclear iron oxygenases in general requires two electrons and protons to facilitate reductive cleavage of the O–O bond and formation of a high-valent iron oxidant.<sup>[1,2]</sup> For enzymes with an iron(III) resting state, the oxidant is postulated to have a formally Fe<sup>V</sup> oxidation state, for example, Fe<sup>IV</sup>(O)(porphyrin radical) for cytochrome P450<sup>[1]</sup> and Fe<sup>V</sup>(O)(OH) for the Rieske dioxygenases.<sup>[2]</sup> On the other hand, enzymes with an iron(II) resting state often require a tetrahydropterin or an  $\alpha$ -keto acid cofactor to form an Fe<sup>IV</sup>(O) intermediate.<sup>[2]</sup> Such intermediates have recently been trapped and characterized for several enzymes.<sup>[3]</sup>

In model nonheme iron systems, there has been significant recent progress in the generation and characterization of Fe<sup>IV</sup>(O) complexes, most of which were prepared by reaction of iron(II) precursors with oxygen-atom donors (e.g., peroxides, peroxy acids, and ArIO).<sup>[4]</sup> The one exception is the formation of [Fe<sup>IV</sup>(O)(TMC)(CH<sub>3</sub>CN)]<sup>2+</sup> (**1**)<sup>[5]</sup> by reaction of its iron(II) precursor with O<sub>2</sub> in the presence of alcohols or

ethers, reported by Nam and co-workers.<sup>[6]</sup> The mechanism for the formation of **1** under these conditions is not well established, but it was postulated to result from O–O bond homolysis of a ( $\mu$ -1,2-peroxo)diiron(III) intermediate, resembling the mechanism postulated for formation of [Fe<sup>IV</sup>(O)(TPP)] by oxygenation of [Fe<sup>II</sup>(TPP)].<sup>[5,7]</sup> In the latter case, coordination of imidazole *trans* to the peroxo ligand promoted oxoiron(IV) formation. By extension, it seems plausible that binding of the added alcohol or ether to iron may also promote the formation of **1**, as [Fe<sup>II</sup>(TMC)(OTf)<sub>2</sub>] in the absence of such additives is air-stable.<sup>[6]</sup> In the course of our work, we appended a pyridine moiety to the TMC framework to obtain the pentadentate ligand TMC-py (Scheme 1). Its



**Scheme 1.** Cyclam ligands used in this study.

iron(II) and oxoiron(IV) complexes were synthesized and structurally characterized. Interestingly, the oxoiron(IV) complex could be generated by oxygenation of the iron(II) complex, but only in the presence of an electron source (BPh<sub>4</sub><sup>−</sup>) and a proton source.

In our initial exploration of the chemistry of **1**, attempts to coordinate pyridine *trans* to the oxo unit by replacement of the MeCN ligand proved to be unsuccessful, perhaps due to the steric constraints imposed by the binding pocket. To enhance the probability of pyridine coordination we synthesized the TMC-py ligand in which one of the TMC methyl groups is replaced by a 2-pyridylmethyl arm and prepared the corresponding iron(II) complex [Fe<sup>II</sup>(TMC-py)]X<sub>2</sub> (**2**(X)<sub>2</sub>; X = OTf or PF<sub>6</sub>). X-ray analysis of single crystals of **2**(PF<sub>6</sub>)<sub>2</sub> obtained from MeCN/MeOH confirmed coordination of TMC-py as a pentadentate ligand (Figure S1 and Table S2, Supporting Information),<sup>[8]</sup> with the cyclam macrocycle adopting a *trans*-I configuration<sup>[9]</sup> and the pyridine residue bound at the apical position of a distorted square pyramid ( $\tau = 0.45^{[10]}$ ).

The reaction of **2** with PhIO in MeCN solution at room temperature gave pale brown-green complex **3** in about 95 %

[\*] Dr. M. Martinho, Prof. Dr. E. Münck  
Department of Chemistry, Carnegie Mellon University  
Pittsburgh, PA 15213 (USA)  
E-mail: emunck@cmu.edu

Dr. J. England, Dr. V. G. Young, Jr., J. R. Frisch, Prof. Dr. L. Que, Jr.  
Department of Chemistry and Center for Metals in Biocatalysis  
University of Minnesota  
207 Pleasant St. SE, Minneapolis, MN 55455 (USA)  
Fax: (+1) 612-624-7029  
E-mail: larryque@umn.edu

Dr. A. Thibon, Dr. R. Guillot, Prof. Dr. J.-J. Girerd, Dr. F. Banse  
Institut de Chimie Moléculaire et des Matériaux d'Orsay  
UMR CNRS 8182, Laboratoire de Chimie Inorganique, Université  
Paris Sud 11, 91405 Orsay Cedex (France)  
Fax: (+33) 1-6915-4754  
E-mail: fredbanse@icmo.u-psud.fr

[\*\*] This work is the result of equal efforts from A.T. and J.E. It was supported by the U.S. National Institutes of Health (GM-33162 to L.Q. and EB-001475 to E.M.) and by the French program "Energie, Conception Durable 2004" (ACI BioCatOx ECD009 to F.B.). Data collection for the X-ray structure of **3**(OTf)<sub>2</sub> was performed at ChemMatCARS Sector 15, which is principally supported by the National Science Foundation/Department of Energy under grant number CHE-0535644. Use of the Advanced Photon Source was supported by the U.S. Department of Energy, Office of Science, Office of Basic Energy Sciences, under Contract No. DE-AC02-06CH11357.

Supporting information for this article is available on the WWW under <http://dx.doi.org/10.1002/anie.200801832>.

yield with  $\lambda_{\text{max}}$  at 834 nm ( $\epsilon_{\text{max}} = 260 \text{ M}^{-1} \text{ cm}^{-1}$ ; Figure 1, left). Complex **3** can also be generated with 3 equiv  $\text{H}_2\text{O}_2$ , but in lower yield (ca. 65 %). The observed near-IR bands are very similar to those of **1**<sup>[11]</sup> and assigned to ligand-field transitions,

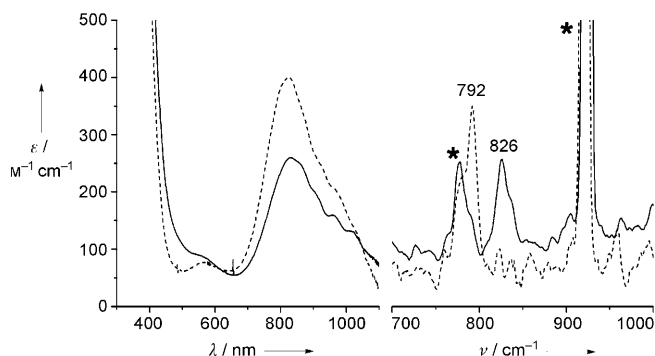


**Figure 1.** Left: electronic spectra of **1** (----) and **3** (—) in MeCN. Right: resonance Raman spectra ( $\lambda_{\text{ex}} = 407 \text{ nm}$ ) of  $^{16}\text{O}$ -**3** (—) and  $^{18}\text{O}$ -**3** (----) recorded in frozen solution with samples mounted on a brass cold finger. Asterisks designate features from the  $\text{CH}_3\text{CN}$  solvent. The Raman samples were prepared by reaction of a 10 mm solution of **2**(OTf)<sub>2</sub> in acetonitrile with 2 equiv of  $\text{PhI}(\text{OAc})_2$ , in the presence of 100 equiv of  $\text{H}_2^{16}\text{O}$  and  $\text{H}_2^{18}\text{O}$ , respectively.

which are diagnostic of the formation of a low-spin ( $S = 1$ ) oxoiron(IV) center.<sup>[12]</sup> Consistent with this assumption, the electrospray mass spectrum of **3** exhibited a peak at  $m/z$  554.1 and an isotope distribution pattern in agreement with its formulation as  $[\{\text{Fe}^{\text{IV}}(\text{O})(\text{TMC-py})\}(\text{OTf})]^+$  (calcd  $m/z$ : 554.2; Figure S2, Supporting Information). Furthermore, the resonance Raman spectrum of **3** showed a  $\nu(\text{Fe}=\text{O})$  band at  $826 \text{ cm}^{-1}$  that shifted by  $34 \text{ cm}^{-1}$  to  $792 \text{ cm}^{-1}$  on  $^{18}\text{O}$  labeling, as expected from Hooke's Law (Figure 1, right). The observed frequency is  $13 \text{ cm}^{-1}$  lower than that observed for **1** by FTIR spectroscopy, and this presumably reflects the differing coordinative properties of axial pyridine and MeCN ligands.<sup>[11]</sup> Mössbauer studies on **3** yielded a doublet with an isomer shift  $\delta$  of  $0.18 \text{ mm s}^{-1}$  and a quadrupole splitting  $\Delta E_Q$  of  $1.08 \text{ mm s}^{-1}$  (Figure 2a), parameters similar to those of **1** ( $\delta = 0.17 \text{ mm s}^{-1}$ ,  $\Delta E_Q = 1.24 \text{ mm s}^{-1}$ ).<sup>[11]</sup> High-field studies (Figure S4, S5, and Table S1, Supporting Information) showed that **3** exhibits zero-field splitting and hyperfine parameters similar to those reported for **1**.<sup>[11]</sup>

The high purity of **3** and its stability ( $t_{1/2} = 7 \text{ h}$  at  $25^\circ\text{C}$ ) allowed the growth of diffraction-quality crystals at  $-20^\circ\text{C}$  from  $\text{MeOH}/\text{Et}_2\text{O}$  (Table S3, Supporting Information). The structure obtained (Figure 3) is only the third high-resolution crystal structure of an oxoiron(IV) complex reported to date<sup>[8]</sup> and conclusively demonstrates that the TMC-py ligand retains its pentadentate binding mode, and the cyclam ring its *trans*-I stereochemistry, on oxidation of **2** to **3**. Complex **3** has an  $\text{Fe}=\text{O}$  distance of  $1.667(3) \text{ \AA}$ , which is  $0.02\text{--}0.03 \text{ \AA}$  longer than those of  $1.646(3) \text{ \AA}$  reported for **1**<sup>[11]</sup> and  $1.639(5) \text{ \AA}$  for  $[\text{Fe}^{\text{IV}}(\text{O})(\text{N4Py})]^{2+}$  (**5**).<sup>[5,13]</sup> The  $\text{Fe}-\text{N}_{\text{amine}}$  bonds in **3** have an average length of  $2.083 \text{ \AA}$ , close to that of **1** ( $2.091 \text{ \AA}$ ). In contrast, the  $\text{Fe}-\text{N}_{\text{py}}$  bond length in **3** is  $2.118(3) \text{ \AA}$ , which is  $0.06 \text{ \AA}$  longer than the axial  $\text{Fe}-\text{N}_{\text{NCMe}}$  bond in **1**,<sup>[11]</sup> despite the fact that pyridine is a much better

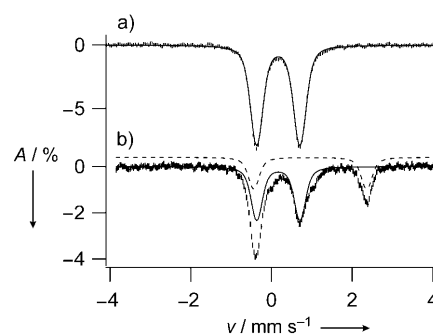


**Figure 2.** Mössbauer spectra recorded at 4.2 K in a parallel applied field of 45 mT for **3** generated a) by treating **2** in MeCN with  $\text{PhIO}$  to afford a sample that contained  $> 95\%$  **3** and b) by treating **2** in MeCN with  $\text{O}_2$  in the presence of 1 equiv  $\text{BPh}_4^-$  and 1 equiv  $\text{HClO}_4$ . Solid and dashed lines indicate contributions of **3** (56% of Fe) and starting material **2** (32%), respectively.

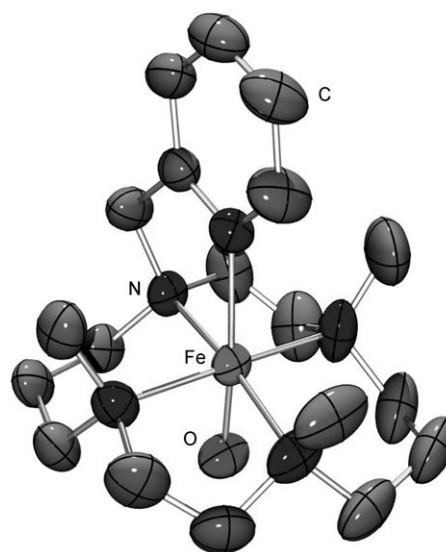


**Figure 3.** Thermal ellipsoid drawing of  $[\text{Fe}^{\text{IV}}(\text{O})(\text{TMC-py})](\text{OTf})_2$  (**3**) showing 50% probability ellipsoids. The second enantiomorph, hydrogen atoms, counterions, and noncoordinating solvent molecules have been omitted for clarity. Selected bond lengths [ $\text{\AA}$ ]:  $\text{Fe}-\text{O}$ ,  $1.667(3)$ ,  $\text{Fe}-\text{N}_{\text{py}}$ ,  $2.118(3)$ ,  $\text{Fe}-\text{N}_{\text{amine}}$  (av)  $2.083$ .

Lewis base than MeCN. This observation may be attributed to the geometric constraints imposed by tethering of the pyridine donor to the cyclam ring, which is also manifested in deviation of the  $\text{O}=\text{Fe}-\text{N}_{\text{py}}$  bond angle from linearity ( $169.77(13)^\circ$ ). Furthermore, the  $\text{Fe}-\text{N}_{\text{py}}$  bond in **3** is significantly longer than the equatorial  $\text{Fe}-\text{N}_{\text{py}}$  bonds of **5** (av  $1.96 \text{ \AA}$ ),<sup>[13]</sup> which most probably reflects the *trans* effect of the oxo ligand. Metrical parameters obtained from a DFT geometry optimization for **3** (Figure S7 and Table S4, Supporting Information) are in good agreement with the X-ray structure. Of particular note is the close reproduction of the nonlinear  $\text{O}=\text{Fe}-\text{N}_{\text{py}}$  bond angle and associated elongation of the  $\text{Fe}-\text{N}_{\text{py}}$  bond length.

The susceptibility of **2** to oxidation by  $\text{O}_2$  was then investigated. While **2** was found to be air-stable at  $25^\circ\text{C}$  in MeCN, it was converted to **3** within minutes in the presence of 1 equiv  $\text{BPh}_4^-$  and 1 equiv  $\text{HClO}_4$ , as indicated by the growth

of the ligand-field band at 834 nm (Figure S3, Supporting Information). The Mössbauer spectrum of a  $^{57}\text{Fe}$ -enriched sample obtained under these conditions (Figure 2b) showed the presence of three components: **3** (56%), unconverted **2** (32%), and an unidentified high-spin ferric byproduct (ca. 12%). Thus, the amount of **3** formed by oxygen activation represented about 80% of the **2** that was oxidized, a yield that is comparable to those for two oxoiron(IV) porphyrin complexes obtained by reductive activation of corresponding oxheme precursors.<sup>[14]</sup>

The yield of **3** obtained by oxygen activation depended on the amount of  $\text{BPh}_4^-$  and  $\text{HClO}_4$  added to the oxygenated solution (Figure 4) and was found to be maximal for samples

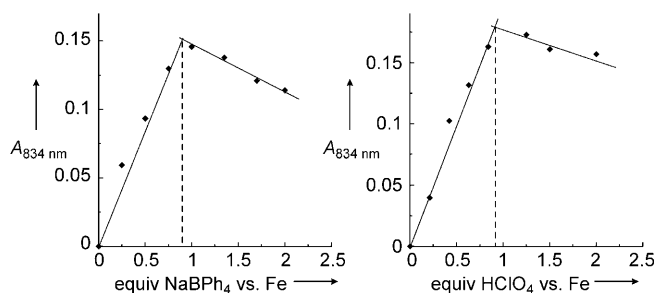
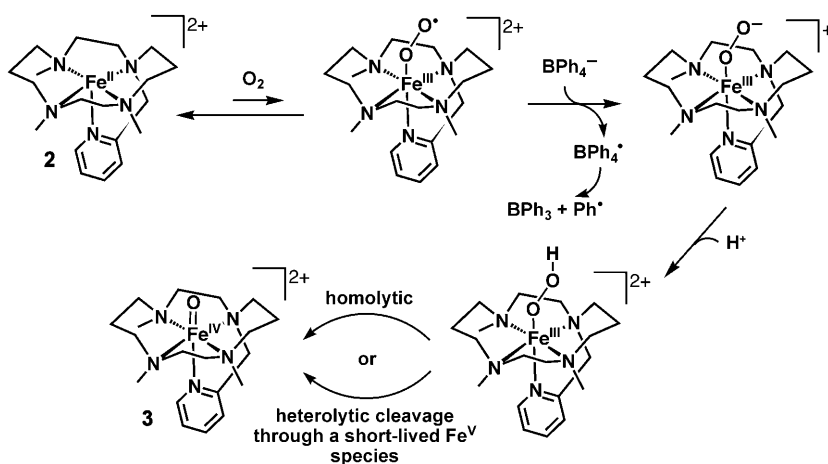


**Figure 4.** Conversion of **2** to **3** by reaction with  $\text{O}_2$  in the presence of  $\text{BPh}_4^-$  and  $\text{H}^+$  in  $\text{CH}_3\text{CN}$  solution at  $25^\circ\text{C}$ . Left: amount of **3** formed as a function of the amount of  $\text{BPh}_4^-$  added to a solution containing 1 equiv of both **2** and  $\text{HClO}_4$ . Right: amount of **3** formed as a function of  $\text{HClO}_4$  added to a solution containing 1 equiv of both **2** and  $\text{BPh}_4^-$ .

containing a 1:1:1 ratio of **2**/ $\text{BPh}_4^-/\text{H}^+$ . Under these conditions, **3** exhibited a four-fold shorter lifetime ( $t_{1/2} \approx 100$  min) than when prepared with  $\text{H}_2\text{O}_2$  or  $\text{PhIO}$ . Studies of the reaction mixture by NMR spectroscopy showed that  $\text{BPh}_4^-$  had decomposed to form phenol (1 equiv) and biphenyl (0.75 equiv) byproducts, presumably derived from phenyl radicals formed on one-electron oxidation of  $\text{BPh}_4^-$ . Thus,  $\text{BPh}_4^-$  acts as a reductant in this reaction.<sup>[15]</sup> Additionally, we also found that ascorbic acid could be used as both an electron and a proton source in the conversion of **2** to **3** and that introduction of 0.5 equiv of ascorbic acid in an ethanol suspension to an oxygenated solution of **2** in a 1:1 mixture of MeCN and EtOH afforded **3** in about 55% yield.

Comparison of the dioxygen reactivity of **2** with that of the precursor to **1**,  $[\text{Fe}^{\text{II}}(\text{TMC})(\text{OTf})](\text{OTf})$  (**4**), reveals similarities and differences. Like **2**, **4** was unreactive towards  $\text{O}_2$  in MeCN solvent at room temperature but was converted to **1** in 75% yield within minutes in the presence of 1 equiv each of  $\text{H}^+$  and  $\text{BPh}_4^-$ . However, unlike **2**, which is air-stable in MeCN/EtOH (1:1), **4** readily reacted with  $\text{O}_2$  to form **1** in nearly quantitative yield in MeCN/EtOH (1:1) and other MeCN/(alcohol or ether) solvent mixtures.<sup>[6]</sup>

In the latter case, Nam and co-workers proposed that dioxygen activation occurs via a (1,2-peroxo)diiron(III) species akin to that proposed for  $\text{Fe}(\text{porphyrin})$  autoxidation,<sup>[7,16]</sup> but no detailed studies substantiating this mechanism have been reported. The fact that dioxygen activation by **4** occurs only in the presence of an alcohol or ether cosolvent raises the possibility that this additive coordinates to the iron(II) center to promote binding and activation of the *trans*-bound  $\text{O}_2$ . Consistent with this notion is the air stability of **2** in MeCN/EtOH (1:1), because **2** differs from **4** in having only one available coordination site, which is presumably reserved for binding of  $\text{O}_2$  and its subsequent activation. In the presence of  $\text{H}^+$  and  $\text{BPh}_4^-$ , we propose instead a reductive activation mechanism for conversion of **2** to **3** (Scheme 2), in which the initially formed  $\text{Fe}^{\text{III}}(\text{OOH})$  intermediate subsequently decomposes rapidly by O–O bond cleavage to form **3**. The O–O bond cleavage may proceed in a homolytic fashion, but we have yet to obtain evidence for formation of a hydroxyl radical. Alternatively, heterolytic cleavage to yield a short-lived oxoiron(V) species, followed by its rapid reduction cannot be ruled out at this stage. Although the proposed  $\text{Fe}^{\text{III}}(\text{OOH})$  intermediate has not to date been observed in the reaction of **2** with dioxygen, our mechanistic proposal is preceded by the trapping and characterization of an  $\text{Fe}^{\text{III}}(\text{OOH})$  species supported by a related pentadentate ligand with amine, pyridine, and pivaloylamido functionalities in the reaction of its iron(II) complex with  $\text{O}_2$  in the presence of  $\text{BPh}_4^-$  and  $\text{H}^+$ .<sup>[17]</sup> This intermediate could alternatively be prepared from the reaction of the same  $\text{Fe}^{\text{II}}$  complex with  $\text{H}_2\text{O}_2$ , which allowed its unambiguous identification.<sup>[18]</sup>



**Scheme 2.** Proposed dioxygen activation mechanism.

In summary, we have described a new oxoiron(IV) complex **3** in terms of its spectroscopic properties and high-resolution crystal structure and have demonstrated its formation by reaction of its iron(II) precursor **2** with oxo-transfer agents or with  $\text{O}_2$  in the presence of a reductant and an acid. In the latter case, the requirement of a proton and an electron source is consistent with the intermediacy of a hydroperoxoiron(III) species, which bears strong parallels to the mechanistic paradigm for formation of high-valent iron

oxo species, as postulated for enzymatic systems such as cytochrome P450 and the Rieske dioxygenases.<sup>[1,2]</sup> Although the mechanism of formation of **3** by reaction of **2** with O<sub>2</sub> requires greater definition and is the subject of ongoing investigations, this study represents the first example in a synthetic system of the activation of dioxygen facilitated by protons and electrons to yield high-valent nonheme iron oxo species.

## Experimental Section

**2(OTf)<sub>2</sub>:** Under argon, a solution of TMC-py (0.50 g, 1.50 mmol) in tetrahydrofuran (10 mL) was added to a stirred solution of Fe(OTf)<sub>2</sub>·(CH<sub>3</sub>CN)<sub>2</sub> (0.62 g, 1.43 mmol) in tetrahydrofuran (10 mL). A precipitate began to form within minutes. After stirring overnight, the volume of solvent was reduced to ca. 10 mL and the mixture filtered. The solid obtained was washed with THF (2 × 5 mL) and dried under vacuum to give the product as a cream-colored powder (0.74 g, 75 %). Elemental analysis (%) calcd for C<sub>21</sub>H<sub>35</sub>F<sub>6</sub>FeN<sub>5</sub>O<sub>8</sub>S<sub>2</sub>: C 36.69, H 5.13, N 10.19; found: C 36.44, H 5.14, N 9.97. **2(PF<sub>6</sub>)<sub>2</sub>** was prepared in a similar fashion. A solution of FeCl<sub>2</sub>·2H<sub>2</sub>O (0.121 g, 0.74 mmol) in MeOH (5 mL) was added to a solution of TMC-py (0.248 g, 0.74 mmol) in minimal MeOH. The yellow solution was stirred overnight and then filtered. Addition of NaPF<sub>6</sub> (0.250 g, 1.49 mmol) in MeOH to the filtrate resulted in formation of a pale precipitate, which was collected by filtration and dried under vacuum to afford the product in 46 % yield. Elemental analysis (%) calcd for C<sub>19</sub>H<sub>35</sub>F<sub>12</sub>FeN<sub>5</sub>P<sub>2</sub>: C 33.59, H 5.19, N 10.31; found: C 33.41, H 5.15, N 9.95.

**3(OTf)<sub>2</sub>:** An excess of solid iodosobenzene was added to a solution of **2(OTf)<sub>2</sub>** in acetonitrile/methanol. After stirring the resultant mixture at room temperature for 20 min, the residual iodosobenzene was removed by filtration to leave an olive-green solution of **3**. Crystals of **3(OTf)<sub>2</sub>** suitable for X-ray crystallography were grown at −20 °C from a methanol solution layered with diethyl ether.

Received: April 19, 2008

Published online: August 4, 2008

**Keywords:** iron · macrocyclic ligands · N ligands · O–O activation · oxo ligands

- [1] M. Sono, M. P. Roach, E. D. Coulter, J. H. Dawson, *Chem. Rev.* **1996**, 96, 2841.
- [2] M. Costas, M. P. Mehn, M. P. Jensen, L. Que, *Chem. Rev.* **2004**, 104, 939.
- [3] C. Krebs, D. Galonic Fujimori, C. T. Walsh, J. M. Bollinger, Jr., *Acc. Chem. Res.* **2007**, 40, 484.
- [4] a) X. Shan, L. Que, Jr., *J. Inorg. Biochem.* **2006**, 100, 421; b) L. Que, Jr., *Acc. Chem. Res.* **2007**, 40, 493.
- [5] Abbreviations: TMC = 1,4,8,11-tetramethyl-1,4,8,11-tetraazacyclotetradecane, TMC-py = 1-(2'-pyridylmethyl)-4,8,11-trimethyl-1,4,8,11-tetraazacyclotetradecane, TPP = dianion of meso-tetraphenylporphyrin, N4Py = N,N-bis(2-pyridylmethyl)-bis(2-pyridyl)methylamine.

- [6] S. O. Kim, C. V. Sastri, M. S. Seo, J. Kim, W. Nam, *J. Am. Chem. Soc.* **2005**, 127, 4178.
- [7] a) D.-H. Chin, A. L. Balch, G. N. La Mar, *J. Am. Chem. Soc.* **1980**, 102, 1446; b) D.-H. Chin, G. N. La Mar, A. L. Balch, *J. Am. Chem. Soc.* **1980**, 102, 4344.
- [8] Single-crystal structure and refinement data for **2(PF<sub>6</sub>)<sub>2</sub>**: C<sub>19</sub>H<sub>35</sub>F<sub>12</sub>FeN<sub>5</sub>P<sub>2</sub>, *M<sub>r</sub>* = 679.31, monoclinic, space group *P*<sub>2</sub>/c, *a* = 9.8438(4), *b* = 9.7471(5), *c* = 28.3527(13) Å, *α* = 90, *β* = 90.803(2), *γ* = 90°, *V* = 2720.1(2) Å<sup>3</sup>, *Z* = 4, *ρ*<sub>calcd</sub> = 1.651 Mg m<sup>−3</sup>, MoK<sub>α</sub> radiation (*λ* = 0.71073 Å, *μ* = 0.771 mm<sup>−1</sup>), *T* = 100(1) K. A total of 48672 (*R*<sub>int</sub> = 0.0468) independent reflections with 2 $\theta$  < 30.71° were collected. The resulting parameters were refined to converge at *R*<sub>1</sub> = 0.0839 (*I* > 2 $\sigma$ (*I*)) for 392 parameters and 8407 independent reflections (*wR*<sub>2</sub> = 0.2237; max./min. residual electron density 0.733/−0.658 e Å<sup>−3</sup>; GOF = 1.074. Single-crystal structure and refinement data for **3(OTf)<sub>2</sub>**: C<sub>22</sub>H<sub>39</sub>F<sub>6</sub>FeN<sub>5</sub>O<sub>8</sub>S<sub>2</sub>, *M<sub>r</sub>* = 735.55, triclinic, space group *P* $\bar{1}$ , *a* = 9.6920(8), *b* = 12.2001(10), *c* = 13.9646(17) Å, *α* = 95.294(4), *β* = 108.020(4), *γ* = 98.922(4)°, *V* = 1533.8(3) Å<sup>3</sup>, *Z* = 2, *ρ*<sub>calcd</sub> = 1.593 Mg m<sup>−3</sup>, synchrotron radiation (*λ* = 0.49594 Å, *μ* = 0.232 mm<sup>−1</sup>), *T* = 100(2) K. A total of 6096 (*R*<sub>int</sub> = 0.0275) independent reflections with 2 $\theta$  < 18.09° were collected. The resulting parameters were refined to converge at *R*<sub>1</sub> = 0.0632 (*I* > 2 $\sigma$ (*I*)) for 627 parameters and 6096 independent reflections (*wR*<sub>2</sub> = 0.1877; max./min. residual electron density 1.150/−0.517 e Å<sup>−3</sup>; GOF = 1.052. Further experimental details are provided in the Supporting Information. CCDC 683058 and 685380 contain the supplementary crystallographic data for this paper. These data can be obtained free of charge from The Cambridge Crystallographic Data Centre via [www.ccdc.cam.ac.uk/data\\_request/cif](http://www.ccdc.cam.ac.uk/data_request/cif).
- [9] B. Bosnich, C. K. Poon, M. L. Tobe, *Inorg. Chem.* **1965**, 4, 1102.
- [10] A. W. Addison, T. N. Rao, J. Reedijk, J. van Pijn, G. C. Verschoor, *J. Chem. Soc. Dalton Trans.* **1984**, 1349.
- [11] J. U. Rohde, J. H. In, M. H. Lim, W. W. Brennessel, M. R. Bukowski, A. Stubna, E. Münck, W. Nam, L. Que, *Science* **2003**, 299, 1037.
- [12] a) A. Decker, J.-U. Rohde, L. Que, Jr., E. I. Solomon, *J. Am. Chem. Soc.* **2004**, 126, 5378; b) A. Decker, J.-U. Rohde, E. J. Klinker, S. D. Wong, L. Que, Jr., E. I. Solomon, *J. Am. Chem. Soc.* **2007**, 129, 15983.
- [13] E. J. Klinker, J. Kaizer, W. W. Brennessel, N. L. Woodrum, C. J. Cramer, L. Que, Jr., *Angew. Chem.* **2005**, 117, 3756; *Angew. Chem. Int. Ed.* **2005**, 44, 3690.
- [14] a) M. Schappacher, R. Weiss, *J. Am. Chem. Soc.* **1985**, 107, 3736; b) D. Mandon, R. Weiss, M. Franke, E. Bill, A. X. Trautwein, *Angew. Chem.* **1989**, 101, 1747; *Angew. Chem. Int. Ed.* **1989**, 28, 1709.
- [15] a) M. G. B. Drew, C. Cairns, S. G. McFall, S. M. Nelson, *J. Chem. Soc. Dalton Trans.* **1980**, 2020; b) P. K. Pal, S. Chowdhury, M. G. B. Drew, D. Datta, *New J. Chem.* **2002**, 26, 367.
- [16] A. L. Balch, Y.-W. Chan, R.-J. Cheng, G. N. La Mar, L. Latos-Grazynski, M. W. Renner, *J. Am. Chem. Soc.* **1984**, 106, 7779; R. A. Ghiladi, R. M. Kretzer, I. Guzei, A. L. Rheingold, Y.-M. Neuhold, K. R. Hatwell, A. D. Zuberbühler, K. D. Karlin, *Inorg. Chem.* **2001**, 40, 5754.
- [17] M. Martinho, Ph.D. thesis, Université Paris Sud 11 (Orsay), **2006**.
- [18] M. Martinho, F. Banse, J. Sainton, C. Philouze, R. Guillot, G. Blain, P. Dorlet, S. Lecomte, J. J. Girerd, *Inorg. Chem.* **2007**, 46, 1709.